Raport Badawczy
Research Report

RB/11/2014

Comparison of inventory maps with independent emission assessments, both for Poland and Ukraine. Steps towards assessment of significance of various activity sources, and validation of emission factors

Z. Nahorski, J. Horabik, J. Jarnicka,
R. Bun, M. Lesiv, O. Danylo

Instytut Badań Systemowych
Polska Akademia Nauk

Systems Research Institute
Polish Academy of Sciences

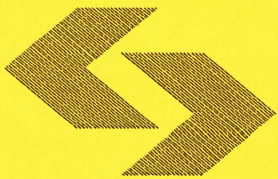

POLSKA AKADEMIA NAUK

Instytut Badań Systemowych

ul. Newelska 6

01-447 Warszawa

tel.: (+48) (22) 3810100

fax: (+48) (22) 3810105

Kierownik Zakładu zgłaszający pracę:
Prof. dr hab. inż. Zbigniew Nahorski

Warszawa 2014

D 3.3

Version	1
Date	20.06.2014
Author	SRI, LPNU
Dissemination level	PP
Document reference	D 3.3

GESAPU

Geoinformation technologies, spatio-temporal approaches, and full carbon account for improving accuracy of GHG inventories

Deliverable 3.3. Comparison of inventory maps with independent emission assessments, both for Poland and Ukraine. Steps towards assessment of significance of various activity sources, and validation of emission factors

Zbigniew Nahorski, Joanna Horabik, Jolanta Jarnicka
Systems Research Institute, Polish Academy of Sciences, Poland

Rostyslav Bun, Myroslava Lesiv, Olha Danylo
Lviv Polytechnic National University, Ukraine;

Delivery Date: M42

Project Duration	24 June 2010 – 23 June 2014 (48 Months)
Coordinator	Systems Research Institute of the Polish Academy of Sciences (SRI)
Work package leader	Systems Research Institute of the Polish Academy of Sciences (SRI)

Disclaimer

All rights reserved

This project is supported by funding by the European Commission: FP7-PEOPLE-2009-IRSES, Project n° 247645.

Project: #247645. Call: FP7-PEOPLE-2009-IRSES, Marie Curie Actions—International Research Staff Exchange Scheme (IRSES).

Work package 3. Improving accuracy of inventories by means of spatio-temporal statistical methods

Deliverable 3.3. Comparison of inventory maps with independent emission assessments, both for Poland and Ukraine. Steps towards assessment of significance of various activity sources, and validation of emission factors.

Content

1. **Review of methods useful in quantification of CO_2 emissions at fine resolution**
   - **1.1 Disaggregation of CO_2 emissions to fine spatial scale**
   - **1.2 Estimation of fossil fuel emission changes from $^{14}CO_2$ observations**
   - **1.3 Atmospheric inversion for estimating CO_2 fluxes**
   - **1.4 Flux tower observations**
2. **Comparison of the developed inventory map with independent emission assessments: nighttime lights**
   - **2.1 ODIAC and GESAPU emission assessments**
   - **2.2 Basic assumptions underlying the two approaches for spatial emission assessment**
   - **2.3 Quantitative comparison of emission maps**
3. **Concluding remarks**

List of figures

Figure 1. ODIAC assessment of fossil fuel CO_2 emissions at the territory of Poland in the original 1km × 1km grid [Gg CO_2]

Figure 2. GESAPU assessment of fossil fuel CO_2 emissions at the territory of Poland in 2km × 2km grid [Gg CO_2]

Figure 3. The difference between GESAPU and ODIAC CO_2 emissions [Gg CO_2]

Figure 4. Histogram (left) and boxplot (right) of differences

Figure 5. Histogram of CO_2 emissions in both inventories

Figure 6. Scatterplot of CO_2 emission values [Gg CO_2]

Figure 7. Fossil fuel CO_2 emissions in Warsaw agglomeration and its surroundings

Figure 8. Fossil fuel CO_2 emissions in the Silesia region

List of tables

Table 1. Methodological assumptions: ODIAC versus GESAPU emission data sets

1. Review of methods useful in quantification of CO_2 emissions at fine resolution

1.1 Disaggregation of CO_2 emissions to fine spatial scale

Quantification of CO_2 emissions at fine spatial (and time) scales is advantageous for many environmental, physical, and socio-economic analyzes; in principle, it can be easily integrated with other data in gridded format. It is especially important for improved assessment of carbon cycle and climate change. Of particular importance are estimations of fossil fuel CO_2 fluxes, which are used to quantitatively estimate CO_2 sources and sinks, see e.g. Battle et al. (2000). A few institutions gather data on emissions from fossil fuels at national levels, like the US Department of Energy Carbon Dioxide Information Analysis Center (CDIAC), Boden et al. (2009), Marland et al. (2008); the International Energy Agency (IEA), IEA (2007). IPCC gathers data from national GHG inventories within the Kyoto Protocol agreement and its continuation, IPCC (1996). British Petroleum company compiled energy statistics, BP (2008), which can be also used to estimate national CO_2 emissions. These data have been used for estimation of global sources and sinks at a regional (e.g. continental) scale, Gurney et al. (2002), Baker et al. (2006), Stephens et al. (2007), Raupach et al. (2007), Canadell et al. (2007), Rivier at al. (2010).

For better assessment of sources and sinks, emission data with improved resolution are needed. Apart from few national high resolution inventories, like the Vulcan inventory compiled for United States with the space resolution 10km ×10km and the time resolution 1 month, and considered to be the most accurate nowadays, Gurney et al. (2009), different disaggregation methods have been used to obtain high-resolution emissions. The most straightforward approach was to disaggregate national emissions proportionally to gridded population information, see e.g. Tans et al. (1990), Andres et al. (1996), Olivier et al. (2005). These data are typically compiled with the resolution $1^0 \times 1^0$ (approximately 100km × 100 km). Their resolution cannot be made much finer, as various emissions, like those from power stations, are not correlated well with population distribution.

This way of disaggregation requires gathering a lot of detailed information on emissions or on activities generating emissions. The better the information that is available, the better the final result becomes. So, the role of institutions gathering and publishing data needed for disaggregation becomes very important in this context.

Another proxy data used for disaggregation are the satellite observations of nighttime lights obtained by the Defense Meteorological Satellite Operational Line Scanner (DMSP-OLS) and released for use by the scientific community, see Huang et al. (2014). Early

experiments, Elvidge et al. (1997), Doll et al. (2000), showed that the CO_2 emissions obtained are underestimated in comparison with the CIDIAC data for most countries. A few improvements have been made. Rayner et al. (2010) used a modified Kaya identity, in which emissions are modeled as a product of aerial population density, per capita economic activity, energy intensity of the economy, and carbon intensity of energy. This formula is used to predict emissions from several sectors, namely energy, manufacturing, transport (broken to land, sea, and air emissions), and other, with 0.25^0 resolution. These prediction are then constrained using observations, which are statistics of national emissions, distribution of nightlights and population. Comparison with the Vulcan inventory showed better performance than the models based only on population or only on nightlight data.

Oda and Maksyutov (2011) extracted emissions from point sources before disaggregating the non-point emissions proportionally to the nightlight distribution, and integrated them again to obtain 1km × 1km emission data. The information on locations of high point sources and their emissions were taken from Carbon Monitoring and Action database (CARMA, http://carma.org), and national emissions were calculated from the BP data on usage of fossil fuels.

Ghosh et al. (2010) investigated two models. In the first one, the correlation between the nighttime lights and the Vulcan data is calculated and then used for other countries. This model did not provide satisfactory results. One of the reason for discrepancies of the nightlight emission estimates was an underestimation of the emissions in the dark areas of the nightlight maps. Then, a second model was developed, in which both nighttime lights and population data were used. The US Environmental Protection Agency (EPA) total CO_2 emission data were used. First, high point (electrical power plant) emissions were subtracted from the original data and the difference (non-utility CO_2 emissions) was disaggregated taking into account both the nighttime lights and population distribution. For this, the nightlight map has been divided into lit areas and dark areas. Secondly, the dark areas were halved, and "mean" aerial emission was calculated dividing total non-utility CO_2 emission by the sum of the lit and halved dark areas. The "total emissions" from the lit areas were calculated multiplying the mean aerial emission by the areas, while those for the dark areas were calculated by multiplying the halved mean aerial emission by the areas. Then, the calculated non-utility CO_2 emissions in the lit areas were distributed proportionally to the nighttime lights, and those in the dark areas proportionally to the population. Finally, point emissions and non-utility emissions were integrated to the final grid.

The most difficult application part of the nighttime lights satellite observations is connected with different habits of using lights in different regions. Usually, less developed regions use less nighttime lights as compared to the use of fossil fuel energy there. It may be

observed not only on a world level, but also between regions of bigger countries, and even districts of big cities, which may become important in case of high resolution of final maps. However, the nightlight maps carry information that can help in disaggregation of national emissions.

Nighttime lights cannot, however, indicate the variability existing among sectors, like residential, commercial, industrial or transportation, at least with a usual observation resolution. But radiation from different sectors do not relate in the same way to the CO_2 emissions. With very high resolutions of the disaggregated emission maps, this effect may introduce biases in estimation.

To find locations of the point sources, databases on world installations, like CARMA, are used. These databases do contain errors. For example, not all existing power plants may be covered and emission estimates may be only approximate. In CARMA, the location of a point source has been inserted based on a postal address, which might be, however, the address of the main office, while the facility location was different, or erroneously assigned to a company with similar or the same name, see discussion in Oda & Maksyutov (2011).

1.2 Estimation of fossil fuel emission changes from $^{14}CO_2$ observations

Emissions (or absorptions) of CO_2 cannot be measured directly in the atmosphere, because it is not possible to distinguish from which source they are released. However, fossil fuel emissions are characterized with a of lack of the ^{14}C isotope. The ^{14}C isotope is produced by cosmic radiation in the upper atmosphere, and then it is transported down and absorbed by living organisms. The ^{14}C isotope decays over a few hundred years (its half-life equals approximately 5700 years), while the fossil fuels come from organisms which lived million up to hundred million years ago. Intensive burning of the fossil fuels dilutes the atmospheric concentration of the ^{14}C isotope (Suess, 1955). This way (lack of) ^{14}C isotope may be used as a tracer of fossil fuel originated CO_2, and the rate of dilution can be used to assess local/regional/global emission of fossil fuel CO_2.

The ^{14}C isotope has not been the only tracer of CO_2 emissions considered. Moreover, SF_6 and CO have been investigated (Turnbull et al., 2006, Gamnitzer et al., 2006; Levin & Karstens, 2007), but ^{14}C has been found to be the most useful and directly available. However, Lopez et al. (2013), used additional tracers of CO, NO_x, and $^{13}CO_2$ besides that of $^{14}CO_2$ to estimate relative fossil fuel (from liquid and gas combustion) and biospheric fossil fuel (from biofuels and human and plant respiration) CO_2 in Paris and got good agreement.

Estimation of the fossil fuel CO_2 basically comes from two mass balance equations, for CO_2 and ^{14}C (or $^{14}CO_2$), which are presented in the concentration form (or more usually the

mixing ratio form; the mixing ratio s is defined as $s = \rho_c/\rho_a$, where ρ_c is a CO_2 density and ρ_a is the air density)

$$CO_2^{obs} = CO_2^{bg} + CO_2^{ff} + CO_2^{bio} + CO_2^{other} \quad (1)$$

$$^{14}C^{obs} = {}^{14}C^{bg} + {}^{14}C^{ff} + {}^{14}C^{bio} + {}^{14}C^{other} \quad (2)$$

where the superscripts stay, respectively, for the

$$\Delta^{14}C = \frac{\left(\frac{^{14}C}{C}\right)_{obs} - \left(\frac{^{14}C}{C}\right)_{abs}}{\left(\frac{^{14}C}{C}\right)_{abs}} \quad (3)$$

where the absolute ($_{abs}$) value is the absolute radiocarbon standard ($1.176 \cdot 10^{-12}$ mol^{14}C/molC), related to oxalic acid activity. Equation (3) is usually expressed in per mill (‰) and written as

$$\Delta^{14}C = \left[\frac{\left(\frac{^{14}C}{C}\right)_{obs}}{\left(\frac{^{14}C}{C}\right)_{abs}} - 1\right] \cdot 1000\ [‰] \quad (4)$$

Equation (2) can be easily transformed to be in the $\Delta^{14}C$ form. Dividing both sides of (2) by $\left(\frac{^{14}C}{C}\right)_{abs}$ and subtracting (1) converted to the equation in C, we get for the left hand side

$$\frac{^{14}C^{obs}}{\left(\frac{^{14}C}{C}\right)_{abs}} - C^{obs} = \left[\frac{\frac{^{14}C^{obs}}{C^{obs}}}{\left(\frac{^{14}C}{C}\right)_{abs}} - 1\right] \cdot C^{obs} = \left[\frac{\left(\frac{^{14}C}{C}\right)_{obs}}{\left(\frac{^{14}C}{C}\right)_{abs}} - 1\right] \cdot C^{obs}$$

By similar transformation of the terms on the right hand side, back conversion of C after square brackets to CO_2 and multiplication of both sides by 1000, we obtain the final equation

$$\Delta^{14}C^{obs}CO_2^{obs} = \Delta^{14}C^{bg}CO_2^{bg} + \Delta^{14}C^{ff}CO_2^{ff} + \Delta^{14}C^{bio}CO_2^{bio} + \Delta^{14}C^{other}CO_2^{other} \quad (2')$$

From (1), the concentration of one component can be calculated and inserted to (2'). The choice of the eliminated component depends in principle on possibility of measuring the values present in the equations, and the case considered. For example, Palstra et al. (2008) and Turnbull et al. (2009) eliminate CO_2^{obs}, while Levin & Rödenbeck (2008) eliminate CO_2^{bio}. Having eliminated CO_2^{obs}, the equation for CO_2^{ff} is found as follows

$$CO_2^{ff} = \frac{(\Delta^{14}C^{obs} - \Delta^{14}C^{bg}) \cdot CO_2^{bg}}{\Delta^{14}C^{ff} - \Delta^{14}C^{obs}} + \frac{(\Delta^{14}C^{obs} - \Delta^{14}C^{bio}) \cdot CO_2^{bio}}{\Delta^{14}C^{ff} - \Delta^{14}C^{obs}} + \frac{(\Delta^{14}C^{obs} - \Delta^{14}C^{other}) \cdot CO_2^{other}}{\Delta^{14}C^{ff} - \Delta^{14}C^{obs}}$$

As the concentration (and mixing ratio) of ^{14}C in the fossil fuel CO_2 is equal to 0, then from (4) we have $\Delta^{14}C^{ff} = -1000$. It is often assumed that CO_2^{other}=0, particularly when a site is far from other sources. However, for greater areas with small biosphere component, the influence of ocean may be important. Some authors have assumed $\Delta^{14}C^{bio} = \Delta^{14}C^{bg}$ (Turnbull et al., 2009) and others $\Delta^{14}C^{bio} = \Delta^{14}C^{obs}$ (Riley et al., 2008;Kuc et al., 2007). Other assumptions

may be appropriate for the area considered, as this methodology can be applied to different scale studies, from the global ones to small-scale, such as flux tower measurements of CO_2.

Many authors discuss assumptions and assess underlying uncertainties. Turnbull et al. (2009) present systematic discussion and quantify uncertainties using modelling and the above equations. Uncertainty of the $\Delta^{14}C^{obs}$ measurements is very important; at best it amounts about 2‰, which gives an uncertainty in CO_2^{ff} of 0.7 ppm for a single measurement (Turnbull et al., 2009). The uncertainty of the monthly mean of $\Delta^{14}C^{obs}$ may be about ±1.5 ppm, and annual mean 0.3-0.45 ppm (Levin & Rödenbeck, 2008).

The choice of place for measurements of background values is another important issue. Since the measurements are usually taken for longer time periods, the background values are taken from observations at high-altitude sites. In Europe, commonly used background observations come from the High Alpine Research station Jungfraujoch at 3450 m a.s.l. in the Swiss Alps. More local sites considered in Europe are the Vermunt station in Austria (1800 m a.s.l.) and the Schauinsland in Germany (1205 m a.s.l.). In Poland, there is an observation site at Kasprowy Wierch (1989 m a.s.l.) in High Tatra Mountains, which can be used as a regional reference station (Kuc et al., 2007). Turnbull et al. (2009) estimate differences of 1-3 ‰ due to the choice of a background site.

Discussion of other uncertainties, particularly in the global modelling, can be found in Turnbull et al. (2009). They estimate that the total uncertainty in the calculation of CO_2^{ff} is about 1 ppm for a single observation.

The resolution of CO_2^{ff} determination depends, first of all, on a spatial scale distribution of $\Delta^{14}C^{ff}$ measurements. The $\Delta^{14}C^{ff}$ measuring observation stations are rather scarce. For example, there are only 10 measurement sites in Europe (Palstra et al., 2008). As a consequence, only rough spatial resolution can result from them. Levin & Rödenbeck (2008) attempted to answer the question of detecting reduction of fossil fuel CO_2 emissions from measurements done in two sites in Germany: at the earlier mentioned Schauinsland station, and in the Suburbs of Heidelberg in upper Rhine valley. The conclusion was that in neither station it was possible to detect a significant decreasing or increasing trend of the fossil fuel component. To test the difference between the means of 5 year base and 5 year commitment periods, they assumed their statistical independence and Gaussian distributions, and then applied a statistical *t*-test. With the 95% confidence level, they found that the changes of emission would have to be larger than 36% to be detectable (with 5% significance) at Schauinsland, and 10% to be detectable in Heildelberg. Rayner at al. (2010) used measurements from 194 stations and results of modelling by a transport model to conclude that this way they can get a reduction of uncertainty on pixel (0.25^0 resolution) level fluxes

about 15%, but a reduction of the uncertainty of national emissions of 70% in their downscaling method.

Much better spatial resolution can be obtained using measurements in plant materials, like corn leaves (Hsueh at al., 2007), rice (Shibata et al., 2005), grape wine ethanol (Burchuladze et al., 1989; Palstra et al., 2008), grass (Quarta et al., 2005; Riley et al., 2008), tree leaves (Levin at al., 1980), and tree rings (Tans et al., 1979; Levin & Kromer, 1997, Babst et al., 2014). Most of them allow only for annual estimation, so measurements have to be done for many years to get longer time series. Only wine ethanol and tree rings enable historical records. This way Palstra et al. (2008) was able to measure ^{14}C in 165 different wines from 32 different regions in 9 different European Countries. These measurements were then compared with those obtained from a regional atmospheric transport model, predicting fossil fuel CO_2 with the resolution 55 km × 55 km, with a good compatibility. Riley et al. (2008) used measurements from winter annual grasses collected at 128 sites across California, USA, to model transport of fossil fuel CO_2 by using a regional transport model with the resolution 36 km × 36 km.

These examples show that, at present, the ^{14}C measurements are not sufficient enough to be useful for high resolution disaggregation of emissions. We admit though, that they can give some constraints or local values, which can be perhaps somehow helpful in checking of disaggregation results, or as an additional information for consideration. However, they may be useful for time disaggregation.

1.3 Atmospheric inversion for estimating CO_2 fluxes

The main idea of the inversion methods is to use measurements in the atmosphere to estimate the fluxes. For this, the Bayes estimator is generally applied (Enting, 2002; Tarantola, 2005). We start with formulation of a model, which is basically used in these methods. A linear model which has been used in the IIASA RAINS project is considered

$$\boldsymbol{y}_{\text{obs}} = \mathbf{H}\boldsymbol{x} + \boldsymbol{\psi} \tag{5}$$

where $\boldsymbol{y}_{\text{obs}}$ is a m-vector of the measured atmospheric concentrations (mixing ratios) in the receptor points, in space and time, above the background value, $\boldsymbol{x}$ is a n-vector of fluxes (emisions) from sources in the region considered, and $\mathbf{H}$ is the matrix, which relates emissions in sources to the measurements. The elements of $m \times n$ matrix $\mathbf{H}$ are computed using a transport model. It is assumed that they are constant in the considered time period, which may be a quite rough approximation. $\boldsymbol{\psi}$ is a m-vector of uncertainties of the relation (5), which is modeled as a random variable with the Gaussian distribution

$$p(\boldsymbol{\psi}) = \left[(2\pi)^m \det \mathbf{C}_y\right]^{-1} \exp\left\{-\frac{1}{2}\boldsymbol{\psi}^T \mathbf{C}_y^{-1}\boldsymbol{\psi}\right\} \tag{6}$$

The real fluxes are unknown but it is assumed that a unsure information $\boldsymbol{x}_{\text{prior}}$ on fluxes is given, so that

$$\boldsymbol{x} = \boldsymbol{x}_{\text{prior}} + \boldsymbol{\vartheta} \tag{7}$$

where again the uncertainty is modeled as a random vector with the Gaussian distribution independent on $p(\boldsymbol{\psi})$

$$p(\boldsymbol{\vartheta}) = [(2\pi)^m \det \mathbf{C}_x]^{-1} \exp\left\{-\tfrac{1}{2}\boldsymbol{\vartheta}^T \mathbf{C}_x^{-1}\boldsymbol{\vartheta}\right\} \tag{8}$$

We are looking for the conditional probability $p(\boldsymbol{x}|\boldsymbol{y}_{\text{obs}})$. From the Bayes theory we have

$$p(\boldsymbol{x}|\boldsymbol{y}_{\text{obs}}) = \frac{p(\boldsymbol{y}_{\text{obs}}|\boldsymbol{x})p(\boldsymbol{x})}{p(\boldsymbol{y}_{\text{obs}})} \tag{9}$$

As the Jacobians in the transformations (5) and (7) equal 1, then

$$p(\boldsymbol{y}_{\text{obs}}|\boldsymbol{x}) = \left[(2\pi)^m \det \mathbf{C}_y\right]^{-1} \exp\left\{-\tfrac{1}{2}(\boldsymbol{y}_{\text{obs}} - \mathbf{H}\boldsymbol{x})^T \mathbf{C}_y^{-1}(\boldsymbol{y}_{\text{obs}} - \mathbf{H}\boldsymbol{x})\right\} \tag{10}$$

$$p(\boldsymbol{x}) = [(2\pi)^m \det \mathbf{C}_x]^{-1} \exp\left\{-\tfrac{1}{2}\left(\boldsymbol{x} - \boldsymbol{x}_{\text{prior}}\right)^T \mathbf{C}_x^{-1}\left(\boldsymbol{x} - \boldsymbol{x}_{\text{prior}}\right)\right\} \tag{11}$$

Thus, the conditional probability $p(\boldsymbol{x}|\boldsymbol{y}_{\text{obs}})$ is proportional to

$$p(\boldsymbol{x}|\boldsymbol{y}_{\text{obs}}) \backsim \exp\left\{-\tfrac{1}{2}\left[(\boldsymbol{y}_{\text{obs}} - \mathbf{H}\boldsymbol{x})^T \mathbf{C}_y^{-1}(\boldsymbol{y}_{\text{obs}} - \mathbf{H}\boldsymbol{x}) + \left(\boldsymbol{x} - \boldsymbol{x}_{\text{prior}}\right)^T \mathbf{C}_x^{-1}\left(\boldsymbol{x} - \boldsymbol{x}_{\text{prior}}\right)\right]\right\} \tag{12}$$

Now, assuming that it is unique, the value $\hat{\boldsymbol{x}}$ which maximizes the above conditional probability is taken as the estimator. Namely, it is the value which minimizes the following cost function

$$J = (\boldsymbol{y}_{\text{obs}} - \mathbf{H}\boldsymbol{x})^T \mathbf{C}_y^{-1}(\boldsymbol{y}_{\text{obs}} - \mathbf{H}\boldsymbol{x}) + \left(\boldsymbol{x} - \boldsymbol{x}_{\text{prior}}\right)^T \mathbf{C}_x^{-1}\left(\boldsymbol{x} - \boldsymbol{x}_{\text{prior}}\right) \tag{13}$$

The above cost function has an appealing interpretation. The final estimate should be as close as possible to the prior estimate (the second summand), and as close as possible agree in prediction of atmospheric concentrations with the measurements (the first summand). The weights of both subcriteria depend inversely on error estimates of the priors and measurements.

For a nonlinear dependence of $\boldsymbol{y}_{\text{obs}}$ on $\boldsymbol{x}$ the cost function has to be in general minimized numerically. For the linear case, as above, the solution can be found analytically. Since the matrices $\mathbf{C}_y$ and $\mathbf{C}_x$ are symmetric, the derivative of J with respect to $\boldsymbol{x}$ becomes

$$\tfrac{1}{2}\frac{dJ}{dx} = -\mathbf{H}^T \mathbf{C}_y^{-1}(\boldsymbol{y}_{\text{obs}} - \mathbf{H}\boldsymbol{x}) + \mathbf{C}_x^{-1}\left(\boldsymbol{x} - \boldsymbol{x}_{\text{prior}}\right) \tag{14}$$

Supposing that the below inverted matrix is nonsingular, the derivative is zero for

$$\hat{\boldsymbol{x}} = \left(\mathbf{H}^T \mathbf{C}_y^{-1}\mathbf{H} + \mathbf{C}_x^{-1}\right)^{-1}\left(\mathbf{H}^T \mathbf{C}_y^{-1}\boldsymbol{y}_{\text{obs}} + \mathbf{C}_x^{-1}\boldsymbol{x}_{\text{prior}}\right) =$$

$$= \left(\mathbf{H}^T \mathbf{C}_y^{-1}\mathbf{H} + \mathbf{C}_x^{-1}\right)^{-1}\left[\mathbf{H}^T \mathbf{C}_y^{-1}\left(\boldsymbol{y}_{\text{obs}} - \mathbf{H}\boldsymbol{x}_{\text{prior}}\right) + \left(\mathbf{H}^T \mathbf{C}_y^{-1}\mathbf{H} + \mathbf{C}_x^{-1}\right)\boldsymbol{x}_{\text{prior}}\right]$$

which finally gives the Bayes estimator of the fluxes

$$\hat{\boldsymbol{x}} = \boldsymbol{x}_{\text{prior}} + \left(\mathbf{H}^T \mathbf{C}_y^{-1}\mathbf{H} + \mathbf{C}_x^{-1}\right)^{-1}\mathbf{H}^T \mathbf{C}_y^{-1}\left(\boldsymbol{y}_{\text{obs}} - \mathbf{H}\boldsymbol{x}_{\text{prior}}\right) \tag{15}$$

If the matrix $\mathbf{H}^T\mathbf{C}_y^{-1}\mathbf{H}+\mathbf{C}_x^{-1}$ is singular, then a singular value decomposition (SVD) can be used.

It can be demonstrated that having inserted $\hat{\boldsymbol{x}}$ to (12) one gets a Gaussian distribution. Then, as the expression under the exponent in a Gaussian distribution is quadratic, we can find the inverse of the covariance matrix $\hat{\mathbf{C}}_x$ of the estimator from the second derivative of J. Differentiating (14) gives

$$\frac{1}{2}\frac{d^2J}{dx^2} = \mathbf{H}^T\mathbf{C}_y^{-1}\mathbf{H} + \mathbf{C}_x^{-1}$$

thus

$$\hat{\mathbf{C}}_x = \left(\mathbf{H}^T\mathbf{C}_y^{-1}\mathbf{H} + \mathbf{C}_x^{-1}\right)^{-1} = \mathbf{C}_x - \mathbf{C}_x\mathbf{H}^T\left(\mathbf{H}\mathbf{C}_x\mathbf{H}^T + \mathbf{C}_y\right)^{-1}\mathbf{H}\mathbf{C}_x \tag{16}$$

This matrix allows us to estimate statistical uncertainty of the Bayesian estimator. The most right expression in (16) is more convenient to be calculated numerically, as only $m \times m$ matrix has to be inverted there, while it is necessary to invert $n \times n$ matrices in the more left expression. Usually, there is $n \gg m$.

Let us look at interpretation of the expressions (15) and (16). The estimate $\hat{\boldsymbol{x}}$ is the sum of the *a priori* estimate plus a correction, which depends on the deviation of observations from their predicted values. This correction improves the initial estimate of fluxes (e.g. obtained from disaggregation of the inventory estimates). The expression (16) tells us that the errors of the improved estimates (the values on the diagonal of $\hat{\mathbf{C}}_x$) are not bigger (and very likely they are smaller) than the errors of the *a priori* estimate.

To use the above expressions, it is necessary to know estimates of the covariance matrices $\hat{\mathbf{C}}_x$ and $\mathbf{C}_y$. This question is discussed in various papers (e.g. Peylin et al., 2005; Rivier et al., 2010; Lauvaux et al., 2008). Different methods of finding appropriate values has been proposed. Very often the diagonal matrices have been used. Exponential decay of covariance values both in space and/or time has been found to better match the reality. Michalak et al. (2005) developed a maximum likelihood method for estimating the covariance parameters. The likelihood function is formulated and the Cramér-Rao bound is derived. However, the likelihood function has to be minimized numerically.

An idea to use the likelihood function approach has been also used in a so-called geostatistical inverse modelling (Gourdji et al., 2008). In this approach, instead of using the prior information, emissions are modeled as linear combinations of trends

$$\boldsymbol{x} = \mathbf{X}\boldsymbol{b} + \boldsymbol{\xi} \tag{17}$$

where $\mathbf{X}$ is a prespecified matrix defining the trends, $\boldsymbol{b}$ is a vector of parameters, and $\boldsymbol{\xi}$ is a vector of errors. The parameters and model structure are estimated using observations $\boldsymbol{y}_{\text{obs}}$ in the relation

$$\boldsymbol{y}_{\text{obs}} = \mathbf{H}\mathbf{X}\boldsymbol{b} + \boldsymbol{\zeta} \tag{18}$$

where $\boldsymbol{\zeta}$ is a linear function of $\boldsymbol{\xi}$ and $\boldsymbol{\psi}$. Looking for a linear estimator

$$\hat{\boldsymbol{z}} = \boldsymbol{\Lambda}\boldsymbol{y}_{\text{obs}} \tag{19}$$

and requiring that it is unbiased, the following equation is obtained

$$(\boldsymbol{\Lambda}\boldsymbol{H}\boldsymbol{X} - \boldsymbol{X})\boldsymbol{b} = \mathbf{0}$$

and it is satisfied when

$$\boldsymbol{\Lambda}\boldsymbol{H}\boldsymbol{X} - \boldsymbol{X} = \mathbf{0} \tag{20}$$

Assuming the Gaussian distributions, maximization of the likelihood function reduces to a minimization of the loss function

$$J_1 = (\boldsymbol{y}_{\text{obs}} - \mathbf{H}\boldsymbol{x})^T \mathbf{C}_y^{-1} (\boldsymbol{y}_{\text{obs}} - \mathbf{H}\boldsymbol{x}) + (\boldsymbol{x} - \mathbf{X}\boldsymbol{b})^T \mathbf{D}_x^{-1} (\boldsymbol{x} - \mathbf{X}\boldsymbol{b}) \tag{21}$$

over $\boldsymbol{x}$ and $\boldsymbol{b}$. Following the geostatistical approach, this minimization is subject to a vector equality constraint (20) coming from the requirement of unbiased prediction by the model. Its solution enables finding the vectors $\hat{\boldsymbol{x}}$ and $\hat{\boldsymbol{b}}$, which minimize the problem, as well as estimates of their covariance matrices. The details are given in Gourdji et al. (2008), and thus are not discussed here.

A more advanced modelling of the fluxes has been proposed in the so called assimilation data method, proposed by Kaminski et al. (2002) and then used e.g. in Rayner et al. (2005). In their method a more thorough model of emissions from the biosphere is included. The models depend on unknown parameters, which are estimated using the Bayesian approach. In place of the simple linear dependence of concentrations (mixing ratios) in the receptor points on fluxes, they use an atmospheric transport model. Then they optimize a cost function of the type

$$J_2 = [\boldsymbol{y}_{\text{obs}} - M(\boldsymbol{p})]^T \mathbf{C}_y^{-1} + \left(\boldsymbol{p} - \boldsymbol{p}_{\text{prior}}\right)^T \mathbf{C}_p^{-1} \left(\boldsymbol{p} - \left(\boldsymbol{x} - \boldsymbol{x}_{\text{prior}}\right)^T \mathbf{C}_x^{-1} \left(\boldsymbol{x} - \boldsymbol{x}_{\text{prior}}\right)\right) \tag{22}$$

where $M(\cdot)$ is the model, $\boldsymbol{p}$ is the vector of parameters, and $\boldsymbol{x}_{\text{prior}}$ is the vector of prior parameter estimates. To minimize this cost function, it is necessary to use a numerical nonlinear optimization method.

The above expressions have been mostly used in flux inversion studies. Ciais et al. (2010) give many comments on practical application of this kind of methods. Peylin et al. (2005) use them for estimating monthly European CO_2 fluxes, and they report 60% reduction of errors. Rivier et al. (2010) applied them for estimating monthly fluxes of CO_2 from the biosphere and ocean for the global and European scale. The Bayesian estimate errors were reduced by 76% of the prior errors for the western and southern Europe, and by 56% for the central Europe. Lauvaux et al. (2008) give inversion results for a 300 km × 300 km region in South-West of France near Bordeaux with the 8 km × 8 km resolution of CO_2 fluxes, with about 50% error reduction. Continuous measurements were taken in two towers, and two

aircraft measuring of CO_2 were used. Thompson et al. (2011) estimated the N_2O fluxes in western and central Europe. With only one in-situ measurement site used for inversion, they obtained between 30% and 60% error reductions for Germany.

The idea of atmospheric inversion methods is actually a general one, and can be used for improving estimates given any additional information in a suitable form. Atmospheric measurements are rather rare in space, so it may be difficult to obtain big improvements at a very fine spatial grid. Perhaps some expectations could be connected with the assimilation data method with a suitable parameterization. Nevertheless, atmospheric inversion methods are nowadays the most important methods used to constrain the emission flux estimates from the biosphere.

A very promising idea is, however, to apply the Bayesian methodology proposed in the atmospheric inversion for combining very high resolution space estimates of the fossil fuel with the information from the nighttime lights. These two information sources give independent information, which can complement each other. In this case, the cost function (13) takes a simpler form

$$J = (\boldsymbol{y}_{\text{obs}} - \boldsymbol{x})^T \mathbf{C}_y^{-1}(\boldsymbol{y}_{\text{obs}} - \boldsymbol{x}) + (\boldsymbol{x} - \boldsymbol{x}_{\text{prior}})^T \mathbf{C}_x^{-1}(\boldsymbol{x} - \boldsymbol{x}_{\text{prior}}) \tag{23}$$

where $\boldsymbol{y}_{\text{obs}}$ is the vector of the emission estimates from the nighttime observations and $\boldsymbol{x}_{\text{prior}}$ is the vector of estimates from disaggregated inventories. The solution of the minimization problem is

$$\hat{\boldsymbol{x}} = \boldsymbol{x}_{\text{prior}} + \left(\mathbf{C}_y^{-1}+\mathbf{C}_x^{-1}\right)^{-1}\mathbf{C}_y^{-1}(\boldsymbol{y}_{\text{obs}} - \boldsymbol{x}_{\text{prior}}) = \boldsymbol{x}_{\text{prior}} + \mathbf{C}_x(\mathbf{C}_y+\mathbf{C}_x)^{-1}(\boldsymbol{y}_{\text{obs}} - \boldsymbol{x}_{\text{prior}}) \tag{24}$$

and the estimate of the improved estimate covariance matrix takes the form

$$\hat{\mathbf{C}}_x = \left(\mathbf{C}_y^{-1} + \mathbf{C}_x^{-1}\right)^{-1} = \mathbf{C}_x - \mathbf{C}_x(\mathbf{C}_x + \mathbf{C}_y)^{-1}\mathbf{C}_x \tag{25}$$

A particularly simple computations are obtained for diagonal covariance matrices $\mathbf{C}_x$ and $\mathbf{C}_y$. In this case the above formulae read

$$\hat{x}_i = x_{i,\text{prior}} + \frac{c_{ii,x}}{c_{ii,x}+c_{ii,y}}(y_{i,\text{obs}} - x_{i,\text{prior}}), \qquad i = 1, \dots, n \tag{26}$$

$$\hat{c}_{ii,x} = \frac{1}{\frac{1}{c_{ii,x}} + \frac{1}{c_{ii,y}}} = \frac{c_{ii,x}c_{ii,y}}{c_{ii,x}+c_{ii,y}}, \qquad i = 1, \dots, n \tag{27}$$

It is readily seen that $\hat{c}_{ii,x} \leq c_{ii,x}$ and $\hat{c}_{ii,x} \leq c_{ii,y}$.

1.4 Flux tower observations

Flux towers offer possibility of direct measurements of emission source and sink fluxes, usually coming from the biosphere. The measurements are done above the plant canopies, and use the so-called eddy covariance method. A basic idea of the eddy covariance is as follows, see also Burba & Anderson (2007).

Let F_z be the vertical flux of a gas. In a turbulent flow, this flux can be presented as

$$F_z = \overline{v\rho_c} = \overline{\rho_a v s} \tag{28}$$

where v is the vertical wind velocity, ρ_c is the gas (CO_2) density, ρ_a is the air density, and $s = \rho_c/\rho_a$ is the earlier introduced mixing ratio. Bar above the variables means averaging over all flows coming from different turbulences (different eddies). Introducing the mean values of each variable (denoted by bar) and its deviation from the means (denoted with Δ before the variable), the above expression can be written as

$$F_z = \overline{(\bar{\rho}_a + \Delta\rho_a)(\bar{v} + \Delta v)(\bar{s} + \Delta s)} =$$

$$= \overline{\bar{\rho}_a\bar{v}\bar{s} + \bar{\rho}_a\bar{v}\Delta s + \bar{\rho}_a\Delta v\bar{s} + \bar{\rho}_a\Delta v\Delta s + \Delta\rho_a\bar{v}\bar{s} + \Delta\rho_a\bar{v}\Delta s + \Delta\rho_a\Delta v\bar{s} + \Delta\rho_a\Delta v\Delta s}$$

But the mean values of deviations equal zero, so we are left with

$$F_z = \overline{\bar{\rho}_a\bar{v}\bar{s} + \bar{\rho}_a\Delta v\Delta s + \Delta\rho_a\bar{v}\Delta s + \Delta\rho_a\Delta v\bar{s} + \Delta\rho_a\Delta v\Delta s}$$

Now, under the assumption that the deviations of the air density are negligible (equal 0), the expression reduces to

$$F_z = \overline{\bar{\rho}_a\bar{v}\bar{s} + \bar{\rho}_a\Delta v\Delta s}$$

Finally, assuming zero average wind velocity, we get

$$F_z = \overline{\bar{\rho}_a\Delta v\Delta s} = \bar{\rho}_a\overline{\Delta v\Delta s} \tag{29}$$

This expression is often further simplified by reducing $\bar{\rho}_a$ with the denominator in the definition of s, to obtain

$$F_z = \overline{\Delta v\Delta\rho_c} = \overline{(v - \bar{v})(\rho_c - \bar{\rho}_c)}$$

In the probability theory, the above expression is the covariance of v and s, from which the name of the method has been coined.

It is further assumed that the stochastic flow processes are ergodic, and then the averaging over the flows is turned over to averaging in time. In practical applications, the means are calculated by averaging the product $\Delta v\Delta s$ for half an hour, and covariances are calculated from very frequent measurements of Δv and Δs (with the frequency 10-20 Hz).

There were many assumptions taken in deriving the formula (29), which may be not satisfied in practical measurements. Foken & Wichura (1996) discuss the errors connected to them.

The flux tower observations could be a perfect way to provide very high resolution emission fluxes from the biosphere both in space and time, provided that a flux tower net is dense enough. Unfortunately, the flux towers are rather scarce. Even in the large area of USA and Canada, only 36 flux tower observations are reported (Raczka et al., 2013). In Poland, there is one experimental flux tower, and in Ukraine there is none. Their use can be therefore considered perhaps in the future, when more flux towers are constructed. At present, they are rather used for an assessment of biosphere emission models, like the one presented in Baldocchi and Meyers (1998) or Raczka et al. (2013).

3. Concluding remarks

A review of available approaches to assimilation of independent emission assessments has been provided. Four groups of methods have been identified, and their basic paradigms and principles have been reviewed. These are: the satellite observations of nighttime lights, the observations of $^{14}CO_2$ mixing ratios, the inversion of atmospheric measurements, and the flux tower observations. An analysis of independent sources of information revealed that, at the present state of availability of observations, only satellite observations of nighttime lights can be readily used for an independent emission assessment of very high resolution inventory, like the one developed for Poland within the GESAPU project. Such data has been received from the ODIAC project. They have been used for a comparison, both in a qualitative and quantitative manner. Regardless of many identified differences in assumptions taken in both methods, a good match was obtained for about 90% of around 80 000 grid cells. The major differences were mainly due to misallocation of some high point sources in the ODIAC data, and due to errors caused by a mismatch in overlay of both maps.

Bibliography

Andres R.J., Marland G., Fung I., Matthews E. (1996) A $1^0 \times 1^0$ distribution of carbon dioxide emissions from fossil fuel consumption and cement manufacture, 1950-1990. *Global Biogeochemical Cycles*, 10:419-429.

Babst F., Alexander M.R., Szejner P., Bouriaud O., Klesse S., Roden J., Ciais P., Poulter B. Frank D., Moore D.J.P., Trouet V. (2014) A tree-ring perspective on the terrestrial carbon cycle. *Oecologia*, (accepted) DOI: 10.1007/s00442-014-3031-6.

Baker D.F., Law R.M., Gurney K.R., Rayner P., Peylin P., Denning A.S., Bousquet P., Bruhwiler L., Vhen Y.H., Ciais P., Fung I.Y., Heimann M., John J., Maki T., Maksyutov S., Masarie K., Prather M., Pak B., Taguchi S., Zhu Z. (2006) TransCom 3 inversion intercomparison: Impact of transport model errors on the interannual variability of regional CO_2 fluxes, 1988-2003. *Global Biogeochemical Cycles*, 20(1), GB10002, DOI: 10.1029/2004GB002439.

Baldocchi D., Meyers T. (1998) On using eco-physiological, micrometeorological and biochemical theory to evaluate carbon dioxide, water vapour and trace gas fluxes over vegetation: a perspective. *Agricultural and Forest Meteorology*, 90:1-25.

Battle M., Bender M.L., Tans P.P., White J.W.C., Ellis J.T., Conway T., Francey R.J. (2000) Global carbon sinks and their variability inferred from atmospheric O_2 and $\delta^{13}C$. *Science*, 287:2467-2470.

Boden T.A., Marland G., Andres R.J. (2010) Global, regional, and national fossil-fuel CO_2 emissions. Carbon Dioxide Information Analysis Center, Oak Ridge National Laboratory, U.S. Department of Energy, Oak Ridge, Tennessee, USA. DOI: 10.3334/CDIAC/00001_V2010.

BP (2014) Statistical Review of World Energy. London. http://www.bp.com/content/dam/bp/pdf/Energy-economics/statistical-review-2014/BP-statistical-review-of-world-energy-2014-full-report.pdf.

Burba G., Anderson D. (2007) Introduction to the Eddy Covariance method: general guidelines and conventional workflow. LI-COR Biosciences, http://www.instrumentalia.com.ar/pdf/Invernadero.pdf

Burchuladze A.A., Chudy M., Eristave I.V., Pagava S.V., Povinec P., Sivo A., Togonidze G.I. (1989) Antropogenic ^{14}C variations in atmospheric CO_2 and wines. *Radiocarbon*, 31(3):771-776.

Canadell J.G., Le Quéré C., Raupach M.R., Field C.B., Buitenhuis E.T., Ciais P., Conway T.J., Gillett N.P., Houghton R.A., Marland G. (2007) Contributions to accelerating atmospheric CO_2 growth from economic activity, carbon intensity, and efficiency of natural sinks. *Proceedings of the National Academy of Sciences*, 104(47):18866-18870, DOI: 10.1073/pnas.0702737104.

Cia P., Rayner P., Chevallier F., Bousquet P., Logan M., Peylin P., Ramonet M. (2010) Atmospheric inversion for estimating CO_2 fluxes: methods and perspectives. *Climatic Change*, 103(1-2):69-92.

Doll C.N.H., Muller J.P., Elvidge C.D. (2000) Nighttime imagery as a tool for global mapping of socioeconomic parameters and greenhouse gas emissions. *Ambio*, 29:157-162.

Elvidge C.D., Baugh K.E., Kihn E.A., Koehl H.W., Davis E.R., Davis C.W. (1997) Relations between satellite observed visible near-infrared emissions, population, economic activity and power consumption. *Remote Sensing*, 18:1373-1379.

Enting I.G. (2002) *Inverse Problems in Atmospheric Constituent Transport*. Cambridge University Press, New York.

Foken T., Wichura B. (1996) Tools for quality assessment of surface-based flux measurements. *Agricultural and Forest Meteorology*, 78:83-105.

Gamnitzer U., Karstens U., Kromer B., Neubert R.E.M., Meijer H.A.J., Schroeder H., Levin I. (2006) Carbon monoxide: A quantitative tracer for fossil fuel CO_2? *Journal of Geophysical Research*, 111, D22302, DOI: 10.1029/2005JD006966.

Ghosh T., Elvidge C.D., Sutton P.C., Baugh K.E., Ziskin D., Tuttle B.T. (2010) Creating a global grid of distributed fossil fuel CO_2 emissions from nighttime satellite imagery. *Energies*, 3:1895-1913, DOI: 10.3390/en312.

Gourdji S.M., Mueller K.L., Schaefer K., Michalak A. (2008) Global monthly averaged CO_2 fluxes recovered using a geostatical inverse modelling approach: 2. Results including auxiliary environmental data. 113, D21115, DOI: 10.1029/JD009733.

Gurney K.R., Rachel L.M., Denning A.S., Rayner P.J., Baker D., Bousquet P., Bruhwiler L., Chen Y.H., Ciais P., Fan S., Fung I.Y., Gloor M., Heimann M., Higuchi K., John J., Maki T., Maksyutov S., Masarie K., Peylin P., Prather M., Pak B.C., Randerson J., Sarmiento J., Taguchi S., Takahashi T., Yuen C.W. ((2002) Towards robust regional estimates of CO_2 sources and sinks using atmospheric transport models. *Nature*, 415:626-630.

Gurney K.R., Mendoza D.L., Zhou Y., Fisher M.L., Miller C.C., Geethakumar S., da la Rue du Can, S. (2009) High resolution fossil fuel combustion CO_2 emission fluxes for the United States. *Environmental Science & Technology*, 43(14):5535-5541, DOI: 10.1021/es900806c.

Hsueh D.Y., Krakauer N.Y., Randerson J.T., Xu X., Trunbore S.E. Southon J.R. (2007)Regional patterns of radiocarbon and fossil fuel-derived CO_2 in surface air across North America. *Geophysical Research Letters*, 34, L02816, DOI: 10.1029/2006GL027032.

Huang Q., Yang X., Gao B, Yang Y., Zhao Y. (2014) Application of DMSP/OLS nighttime light images: A meta-analysis and a systematic literature review. *Remote Sensing*, 6:6844-6866, DOI: 10.3390/rs6086844.

IEA (2007) CO_2 emissions from fuel combustion: 1971-2005. International Energy Agency, Paris, France.

IPCC (1996) Revised IPCCC 1996 guidelines for national greenhouse gas inventories. Technical Report IPCC/OECD/IEA, Paris. http://www.ipcc-nggip.iges.or.jp/public/gl/invsl.html.

Karlen I., Olsson I.U., Kilburg P., Kilici S. (1968) Absolute determination of the activity of two ^{14}C dating standards. *Arkiv Geophysik*, 4:465-471.

Kuc T., Rozanski K., Zimnoch M., Necki J., Chmura L., Jelen D. (2007) Two decades of regular observations of $^{14}CO_2$ and $^{13}CO_2$ content in atmosphere carbon dioxide in Central Europe: Long-term changes of regional anthropogenic fossil CO_2 emissions. *Radiocarbon*, 49(2):807-816.

Lauvaux T., Uliasz M., Sarrat C., Chevallier F., Bousquet P., Lac C., Davis K.J., Ciais P., Denning A.S., Rayner P.J. (2008) Mesoscale inversion: first results from the CERES campaign with synthetic data. *Atmospheric Chemistry and Physics*, 8:3459-3471.

Levin I., Karstens U. (2007) Inferring high-resolution fossil fuel CO_2 records at continental sites from combined $^{14}CO_2$ and CO observations. *Tellus, Ser. B*, 59:245-250.

Levin I., Kromer B. (1997) Twenty years of atmospheric $^{14}CO_2$ observations at Schauinsland station, Germany. *Radiocarbon*, 39(2):205-218.

Levin I., Münnich K.O., Weiss W. (1980) The effect of anthropogenic CO_2 and ^{14}C sources on the distribution of ^{14}C sources on the distribution of ^{14}C in the atmosphere. *Radiocarbon*, 22:379-391.

Levin I., Rödenbeck C. (2008) Can the envisaged reductions of fossil fuel CO_2 emissions be detected by atmospheric observations? *Naturwissenshaften*, 95:203-208, DOI: 10.1007/s00114-007-0313-4.

Marland G., Boden T.A., Andres R.J. (2008) Global, regional, and national fossil fuel CO_2 emissions. In: *Trends: A Compendium of Data on Global Change*, Carbon Dioxide Information Analysis Center. Oak Ridge National Laboratory, Oak Ridge, Tennessee, USA.

Meijer H.A.J., Smid H.M., Perez E., Keizer M.G. (1996) Isotopic characterisation of anthropogenic CO_2 emissions using isotopic and radiocarbon analysis. *Physics and Chemistry of the Earth*, 21(5-6):483-487.

Michalak A., Hirsch A., Bruhwiler L., Gurney K.R., Peters W., Tans P.P. (2005) Maximum likelihood estimation of covariance parameters for Bayesian atmospheric trace gas surface flux inversion. *Journal of Geophysical Research*, 110, D24107, DOI: 10.1029/2005JD005970.

Oda T., Maksyutov S. (2011) A very high-resolution (1 km × 1 km) global fossil fuel CO_2 emission inventory derived using a point source database and satellite observations of nighttime lights. *Atmospheric Chemistry and Physics*, 11:543-556, DOI: 10.5194/acp-11-543-2011.

Olivier J.G.J., Aardenne J.A.V., Dentener F.J., Pagliari V., Ganzeveld L.N., Peters J.A.H.W. (2005) Recent trends in global greenhouse gas emissions: Regional trends 1970-2000 and spatial distribution of key sources in 2000. *Environmental Sciences*, 2(2-3):81-99, DOI: 10.1080/15693430500400345.

Palstra S.W., Karstens U., Streurman H.J., Meijer H.A.J. (2008) Wine ^{14}C as a tracer for fossil fuel CO_2 emissions in Europe: Measurements and model comparison. *Journal of Geophysical Research*, 113, D21305, DOI: 10.1029/2008JD010282.

Peylin P., Rayner P.J., Bousquet P., Carouge C., Hourdin F., Heinrich P., Ciais P., AEROCARB contributors (2005) Daily CO_2 flux estimates over Europe from continuous atmospheric measurements: 1, inverse methodology. *Atmospheric Chemistry and Physics*, 5:3173-3186.

Quarta G., D'Elia M., Rizzo G.A., Calganile L. (2005) Radiocarbon dilution effects induced by industrial settlements in southern Italy. *Nuclear Instruments and Methods in Physics Research, Sec. B*, 240:458-462.

Raczka B.M., Davis K.J., Hutzinger D., Neilson R.P., Poulter B., Richardson A.D., Xiao J., Baker I., Ciais P., Keenan T.F., Law B., Post W.M., Ricciuto D., Schaefer K., Tian H., Tomelleri E., Verbeeck H., Viovy N. (2013) Evaluation of continental carbon cycle simulations with North American flux tower observations. *Ecological Monographs*. 83(4):531-556.

Raupach M.R., Marland G., Ciais P., Le Quéré C., Canadell J.G., Klepper G., Field C.B. (2007) Global and regional drivers of accelerating CO_2 emissions. *Proceedings of the National Academy of Sciences*, 104(24):10288-10293, DOI: 10.1073/pnas.0700609104.

Rayner P.J., Scholze M., Knorr W., Kaminski T., Giering R., Widmann H. (2005) Two decades of terrestrial carbon fluxes from a carbon cycle data assimilation system (CCDAS). *Global Biogeochemical Cycles*, 19, GB2026, DOI: 10.1029/2004GB002254.

Rayner P.J., Raupach M.R., Paget M., Peylin P., Koffi E. (2010) A new global gridded dataset if CO_2 emissions from fossil fuel combustion: Methodology and evaluation. *Journal of Geophysical Research*, 115, D19306, DOI: 10.1029/2009JD013439.

Riley W.G., Hsueh D.Y., Randerson J.T., Fischer M.L., Hatch J., Pataki D.E.,Wang W., Goulden M.L. (2008) Where do fossil fuel carbon dioxide emissions from California go? An analysis based on radiocarbon observations and an atmospheric transport model. *Journal of Geophysical Research*, 113, G04002, DOI: 10.1029/2007JG000625.

Rivier L., Peylin P., Ciais P., Gloor M., Rödenbeck C., Geels C., Karstens U., Bousquet P., Brandt J., Heimann M., Aerocarb experimentalists (2010) European CO_2 fluxes from atmospheric inversions using regional and global transport models. *Climatic Change*, 103(1-2):93-115.

Shibata S., Kawano E., Nakabayashi T. (2005) Atmospheric $[^{14}C]CO_2$ variantions in Japan during 1982-1999 based on ^{14}C measurements in rice grains. *Applied Radiation and Isotopes*, 63:285-290.

Stephens B.B., Gurney K.R., Tans P.P., Sweeney C., Peters W., Bruhwiler L., Cias P., Ramonet M., Bousquet P., Nakazawa T., Aoki S., Innoue T.M.G., Vinnichenko N., Lloyd J., Jordan A., Heimann M., Shibistova O., Langefelds R.L., Steele L.P., Francey R.J., Denning A.S. (2007) Weak northern and strong tropical land carbon uptake from vertical profiles of atmospheric CO_2. *Science*, 316:1732-1735.

Stuiver M., Polach H.A. (1977) Discussion. Reporting of ^{14}C data. *Radiocarbon*, 19(3):355-363.

Suess H.E. (1955) Radiocarbon concentration in modern wood. *Science*, 122:415-417, DOI: 10.1126/science.122.3166.415-a.

Tans P.P., se Jong A.F.M., Mook W.G. (1979) Natural atmospheric ^{14}C variation and the Suess effect. *Nature*, 208:826-828.

Tans P.P, Fung I.Y., Takahashi T. (1990) Observational constraints on the global atmospheric CO_2 budget. *Science*, 247:1431-1438.

Tarantola A. (2005) *Inverse Problem Theory and Methods for Model Parameter Estimation.* SIAM, Philadelphia.

Thompson R.L., Gerbig C., Rödenbeck C. (2011) A Bayesian inversion estimate of N_2O emissions for western and central Europe and the assessment of aggregation error. *Atmospheric Chemistry and Physics*, 11:3443-3458, DOI: 10.5194/acp-11-3443-2011.

Turnbull J.C., Miller J.B., Lehman S.J., Tans P.P., Sparks R.J. (2006) Comparison of $^{14}CO_2$, CO and SF_6 as tracers for recently added fossil fuel CO_2 in the atmosphere and implications for biological CO_2 exchange. *Geophysical Research Letters*, 33, L01817, DOI: 10.1029/2005GL024213.

Turnbull J., Rayner P., Miller J., Naegler T. Ciais P., Cozic A. (2009) On the use of $^{14}CO_2$ as a tracer for fossil fuel CO_2: Quantifying uncertainties using an atmospheric transport model. *Journal of Geophysical Research*, 14:D22302, DOI: 10.1029/2009JD012308.

Zondervan A., Meijer H.A.J. (1996) Isotopic characterization of CO_2 sources during regional pollution events using isotopic and radiocarbon analysis. *Tellus, Ser. B*, 48:601-612.